A Generic Method for the Determination of Non-Detection Zones in DER-Dominated Distribution Grids

Yan Li[1], Peng Zhang[1], Joseph N. Debs[2], David A. Ferrante[2],
Donald J. Kane[2], Samuel N. Woolard[2], Roderick S. Kalbfleisch[2], and Kenneth B. Bowes[2]
[1]Dept. of Electrical and Computer Engineering, University of Connecticut, Storrs, CT 06269-4157, USA
[2]Eversource Energy, Berlin, CT 06037, USA

***Abstract*—Efficiently calculating non-detection zones (NDZ) becomes increasingly important when evaluating unintentional islanding risks of distribution grids that are highly integrated with distributed energy resources (DER). In this paper, a rigorous theoretical method, the DER-Driven Non-Detection Zone (D^2NDZ), is presented to estimate NDZ for any given distribution feeders. Numerical examples indicate that by using D^2NDZ, NDZ can be quickly and effectively obtained while avoiding numerous and time-consuming electromagnetic transient simulations. Therefore, D^2NDZ offers utilities engineers a powerful tool to better understand and operate their systems.**

***Index Terms*—Distribute energy resource (DER), DER-driven non-detection zone, IEEE Standard 1547**

I. Introduction

Though emerging distributed energy resources (DERs) enable reliable power distribution grids, they also introduce some concerns. One major challenge that utilities companies face is the risk of a feeder's unintentional islanding, which can create safety hazards for utility customers and field crews [1]. Unintentional islanding happens when DERs are connected to a feeder that mimics grid conditions, resulting in DERs' anti-islanding algorithms being deceived into staying online even when system faults occur. This challenge rapidly escalates with the trend of more frequent storm-induced blackouts where DERs may continue to energize a power line from customers' homes or businesses. A pressing question to be addressed for distribution planning and operations is how to reliably assess this unintentional islanding risk of an arbitrary feeder in cases of high-DER penetration scenarios. To assess the risk of unintentional islanding, a non-detectional zone (NDZ) can be adopted as a practical metric. This zone refers to the range of operational conditions in which anti-islanding schemes fail to detect abnormal modes [2].

There exist two main categories of NDZ calculation: active detection and passive detection. Active approaches (e.g., active frequency drift [3], Sandia frequency shift [4], voltage shift [5], and reactive power disturbance [6]) have fast responses while causing perturbations in the distribution systems. Passive approaches (e.g., Bayesian passive method [7], over/under frequency [8], over/under voltage [8], pattern recognition [9], and phase jump detection [10]) do not disturb the system while generating a more conservative NDZ than active methods. Examining NDZ under the deep integration of DERs in large distribution grids, however, remains an open challenge.

This material is based upon work supported by Eversource Energy Center under Grant No. 6367940.

To overcome the limitations of existing technologies, a DER-driven non-detection zone (D^2NDZ) evaluation method is developed to effectively estimate the NDZ in distribution networks with a deep integration of DERs. Our main contributions are three-fold: (*i*) D^2NDZ incorporates both the steady-state and dynamic impacts of different types of DER units. (*ii*) D^2NDZ enables quick and effective NDZ estimation without precise electromagnetic transients simulations. (*iii*) D^2NDZ can potentially be developed and implemented online to facilitate distribution grids' operation.

The remainder of this paper is organized as follows: Section II establishes the methodological foundations for this study. The impacts of the steady-state and the dynamics of DERs are rigorously derived, and then the parameters involved in D^2NDZ are obtained via solving an optimization problem. In Section III, tests on Eversource Energy's distribution feeders verify the effectiveness and scalability of D^2NDZ. Conclusions are drawn in Section IV.

II. Methodology of D^2NDZ

Since the boundary of NDZ is identified via several critical operating points of a system, the basic idea of D^2NDZ is to efficiently figure out this boundary by combining a theoretical analysis of the steady state of a generic system with the learning-based dynamic impact of DERs on a system. Specifically, it includes that (1) a primary NDZ considering different types of loads is analytically determined based on the steady state of a system after islanding and (2) the dynamic impact of DERs on the boundary of a primary NDZ is then analyzed and integrated into the primary NDZ to obtain the desired result. A generic system is shown in Fig. 1 to illustrate the NDZ study.

Then the above-mentioned idea of D^2NDZ can be expressed in the following equations, which describe the active power

978-1-5386-7703-2/18/$31.00 ©2018 IEEE

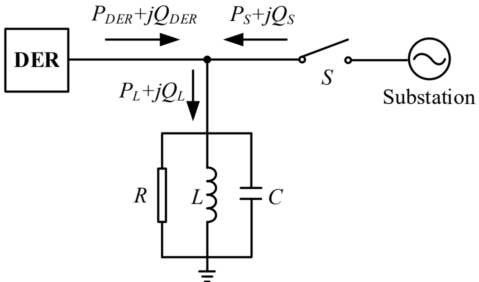

Fig. 1 A schematic distribution feeder showing aggregated load and DER

and reactive power threshold, respectively. All of the expressions will be discussed in the following section.

$$\left.\frac{P_{DER}}{P_L}\right|_{min}^{S}+\left.\frac{P_{DER}}{P_L}\right|_{min}^{D}\leq\frac{P_{DER}}{P_L}\leq\left.\frac{P_{DER}}{P_L}\right|_{max}^{S}+\left.\frac{P_{DER}}{P_L}\right|_{max}^{D}\quad, \quad (1)$$

$$\left.\frac{Q_{DER}}{Q_L}\right|_{min}^{S}+\left.\frac{Q_{DER}}{Q_L}\right|_{min}^{D}\leq\frac{Q_{DER}}{Q_L}\leq\left.\frac{Q_{DER}}{Q_L}\right|_{max}^{S}+\left.\frac{Q_{DER}}{Q_L}\right|_{max}^{D}\quad, \quad (2)$$

where P_{DER}, Q_{DER} represent the active and reactive power injection from DER units; $\left.\frac{P_{DER}}{P_L}\right|_{min}^{S}$, $\left.\frac{P_{DER}}{P_L}\right|_{max}^{S}$ represent the lower and upper bounds of the ratio of active power to active load when only the steady state is considered; $\left.\frac{Q_{DER}}{Q_L}\right|_{min}^{S}$, $\left.\frac{Q_{DER}}{Q_L}\right|_{max}^{S}$ represent the lower and upper bounds of the ratio of reactive power to reactive load when only the steady state is considered; $\left.\frac{P_{DER}}{P_L}\right|_{min}^{D}$, $\left.\frac{P_{DER}}{P_L}\right|_{max}^{D}$ represent the impacts of DER dynamics on the lower and upper bounds of the ratio of active power to active load; $\left.\frac{Q_{DER}}{Q_L}\right|_{min}^{D}$, $\left.\frac{Q_{DER}}{Q_L}\right|_{max}^{D}$ represent the impacts of DER dynamics on the lower and upper bounds of the ratio of reactive power to reactive load. Our task, therefore, is to identify such a zone that closely approximates the actual NDZ.

A. *Derivation of the Primary Non-Detection Zone*

1) Ratio Bounds of Active Power to Active Load: Islanding detection normally takes only a few cycles, whereas DER units such as a PV array and wind turbine generators usually operate at maximum power points that do not change instantaneously. This means that DER power outputs can be treated as constants during islanding detection. Therefore, the active power consumption along the feeder before and after islanding (circuit breaker S tripped off and switched on) can be expressed by (3) and (4), respectively [2].

$$P_L=P_{DER}+P_S=\frac{V^2}{R}, \quad (3)$$

$$P_{DER}=\frac{(V+\Delta V)^2}{R+\Delta R}, \quad (4)$$

where P_L is the active load, P_S is the active power obtained from the substation, V the positive sequence voltage magnitude before islanding, ΔV is the voltage deviation after islanding, and ΔR is the resistance change after islanding. As a result, the ratio of active power to active load due to steady-state conditions can be expressed as

$$\left.\frac{P_{DER}}{P_L}\right|^{S}=\frac{(V+\Delta V)^2}{V^2}\cdot\frac{R}{R+\Delta R}=(1+\mu)^2\cdot\frac{1}{1+\frac{\Delta R}{R}}, \quad (5)$$

where $\mu=\Delta V/V$ represents the voltage deviation. Then through further derivation on the resistance change after islanding, the following expression can be obtained:

$$\frac{\Delta R}{R}=\frac{\Delta R_P+\Delta R_C}{R_I+R_P+R_C}=\frac{(2\mu+\mu^2)P_IP_C+\mu P_IP_P}{P_IP_C+P_IP_P+P_PP_C}, \quad (6)$$

where R_I, R_P, R_C represent the real part of constant impedance, constant power and constant current loads before islanding, respectively; ΔR_I, ΔR_P, ΔR_C represent the incremental resistive portions in constant impedance, power and current loads after islanding, with their expressions given in the Appendix; P_I, P_P, P_C are the percentages of constant impedance, constant power and constant current loads, respectively. Substituting (6) into (5), the ratio of active power to active load can be rewritten as

$$\begin{aligned}\left.\frac{P_{DER}}{P_L}\right|^{S}&=\frac{(1+\mu)^2(P_IP_C+P_IP_P+P_PP_C)}{(1+\mu)^2P_IP_C+(1+\mu)P_IP_P+P_PP_C}\\&=f(\mu,P_I,P_P,P_C). \quad (7)\end{aligned}$$

Consequently, by considering the voltage deviation bounds within which an island may not be detected (see IEEE Standard 1547-2003 [11]), the ratio bounds of active power to active load $\left.\frac{P_{DER}}{P_L}\right|_{min}^{S}$ and $\left.\frac{P_{DER}}{P_L}\right|_{max}^{S}$ can be evaluated by

$$\left.\frac{P_{DER}}{P_L}\right|_{min}^{S}=\min f(\mu,P_I,P_P,P_C), \quad (8)$$

$$\left.\frac{P_{DER}}{P_L}\right|_{max}^{S}=\max f(\mu,P_I,P_P,P_C), \quad (9)$$

where $min()$ and $max()$ are functions to get the minimum and maximum values, respectively.

From (8) and (9), it can be seen that the ratio of active power to active load mainly depends on the deviation of voltage and the components of load.

2) Ratio Bounds of Reactive Power to Reactive Load: The reactive power consumed in the feeder load before and after islanding can be formulated in (10) and (11), respectively.

$$Q_L=Q_{DER}+Q_S=V^2\left(\frac{1}{2\pi fL}-2\pi fC\right), \quad (10)$$

$$\begin{aligned}Q_{DER}=(V+\Delta V)^2\Big(&\frac{1}{2\pi(f+\Delta f)(L+\Delta L)}\\&-2\pi(f+\Delta f)(C+\Delta C)\Big). \quad (11)\end{aligned}$$

where f represents the system frequency, Δf represents the frequency deviation after islanding, ΔC represents the capacitor deviation after islanding, and ΔL represents the inductance deviation after islanding.

Thus, the ratio of reactive power to reactive load due to steady-state conditions can be expressed as

$$\frac{Q_{DER}}{Q_L}\bigg|^S = (1+\mu)^2\bigg(\frac{1}{2\pi(f+\Delta f)(L+\Delta L)} -2\pi(f+\Delta f)(C+\Delta C)\bigg)/\bigg(\frac{1}{2\pi f L}-2\pi f C\bigg) \tag{12}$$

Assuming the variations in load inductance and capacitance are small before and after islanding, the following equations can be obtained,

$$\Delta L\cdot\Delta C \approx 0, \tag{13}$$
$$1+\frac{\Delta L}{L}\approx 1, \tag{14}$$
$$1+\frac{\Delta C}{C}\approx 1. \tag{15}$$

Then (12) can be re-formulated as

$$\frac{Q_{DER}}{Q_L}\bigg|^S = (1+\mu)^2(1+\rho) = g(\mu,\rho), \tag{16}$$

where $\rho = \Delta f/f$ is the frequency deviation after islanding.

Consequently, by considering the voltage and frequency deviation bounds within which an island may not be detected [11], the ratio bounds of reactive power to reactive load $\frac{Q_{DER}}{Q_L}\big|^S_{min}$ and $\frac{Q_{DER}}{Q_L}\big|^S_{max}$ can be obtained by

$$\frac{Q_{DER}}{Q_L}\bigg|^S_{min} = \min g(\mu,\rho), \tag{17}$$
$$\frac{Q_{DER}}{Q_L}\bigg|^S_{max} = \max g(\mu,\rho). \tag{18}$$

From (17) and (18), it can be seen that the ratio of reactive power to reactive load mainly depends on the deviation of voltage and frequency after islanding.

Note that R/X ratio is not involved in the above derivation, which means this generic method is not limited to the ratio value of R/X.

B. Non-Detection Zone Bounds Driven by DER Dynamics

Besides the steady state behaviors, the transient processes of the DER units also significantly impact NDZ, especially on its boundary. In order to incorporate this effect, first, electromagnetic transients (EMT) simulations are carried out in various distribution feeders to provide experimental data. These results are then analyzed and learned to develop a generic formulation which is used to augment the primary NDZ. Deep integration of PVs is given as an example and analyzed in detail. Other types of DERs can be models in the D^{2}NDZ study following the same procedure.

1) Impact of DER Dynamics on the Ratio Bounds of Active Power to Active Load: Experimental results obtained from EMT simulations show that, the more maximum power point tracking (MPPT) controlled PV units a system has, the more compact the NDZ will be. The reason is analyzed as follows: The MPPT control systems of PV arrays connected to a feeder must be properly coordinated to enable a transition from the grid-connected mode to the islanded mode. In practice, it is very difficult to achieve this goal when multiple MPPT controlled PV units are integrated at different locations without communication. This exponentially reduces the size of the NDZ when there is a deep integration of PV units. In this paper, therefore, the following exponential model is established to characterize the impact of PV dynamics on NDZ.

$$\phi_{PV,L} = \beta_{PV,L}(1-\alpha_{PV,L}\mathrm{e}^{-N_{PV}}), \tag{19}$$
$$\phi_{PV,H} = \beta_{PV,H}(1-\alpha_{PV,H}\mathrm{e}^{-N_{PV}}), \tag{20}$$

where $e^{(\cdot)}$ means the exponential function; coefficients $\beta_{PV,L}, \alpha_{PV,L}, \beta_{PV,H}, \alpha_{PV,H}$ can be determined by learning the experimental data. Note that, after $\beta_{PV,L}$ and $\beta_{PV,H}$ are determined, they should be updated by multiplying a coefficient to always ensure a conservative NDZ estimation.

Therefore, other types of DERs can also be modeled following the process outlined above. Assume their impacts on the lower and upper ratio bounds can be expressed as h_L and h_H, respectively. The overall impact of DER dynamics on the lower and upper ratio bounds of active power to active load can be expressed as a weighted sum of individual contributions from different types of DERs shown as follows:

$$\frac{P_{DER}}{P_L}\bigg|^D_{min} = \delta_{PV}\phi_{PV,L} + \delta_h h_L, \tag{21}$$
$$\frac{P_{DER}}{P_L}\bigg|^D_{max} = \delta_{PV}\phi_{PV,H} + \delta_h h_H, \tag{22}$$

where δ_{PV} and δ_h are Kronecker signs.

2) Impact of DER Dynamics on the Ratio Bounds of Reactive Power to Reactive Load: Similar to the analysis above, the overall impact of DER dynamics on the lower and upper ratio bounds of reactive power to reactive load can be presented by a weighted sum of the contributions from each type of DERs, as shown below

$$\frac{Q_{DER}}{Q_L}\bigg|^D_{min} = \delta_{PV}\varphi_{PV,L} + \delta_h l_L, \tag{23}$$
$$\frac{Q_{DER}}{Q_L}\bigg|^D_{max} = \delta_{PV}\varphi_{PV,H} + \delta_h l_H, \tag{24}$$

where the contributing factors are given by

$$\varphi_{PV,L} = \gamma_{PV,L}(1-\eta_{PV,L}\mathrm{e}^{-N_{PV}}), \tag{25}$$
$$\varphi_{PV,H} = \gamma_{PV,H}(1-\eta_{PV,H}\mathrm{e}^{-N_{PV}}). \tag{26}$$

3) Parameter Determination: As an estimation method, the performance of D^{2}NDZ mainly depends on the parameters in each formula, e.g., $\alpha_{PV,L}$, $\alpha_{PV,H}$, etc. In this paper, sequential quadratic programming (SQP) is used to optimize these parameters from the experiments' data. Specifically, the parameters of D^{2}NDZ are formulated into four independent optimization problems. For instance, (27) shows the optimization formulation for identifying the parameters that determine the lower ratio bound of active power to active load.

$$\begin{cases} \min f = \sum_{i=1}^{N_C} m_i \left(\frac{P_{DER}}{P_L}\Big|_{min,i} (\beta_{PV,L}, \alpha_{PV,L}) - \frac{P_{DER}}{P_L}\Big|_{min,i}^{E} \right)^2 \\ s.t. \quad \beta_{PV,L} \in \mathbb{R}, \alpha_{PV,L} \in \mathbb{R}, \end{cases} \tag{27}$$

where $\frac{P_{DER}}{P_L}\Big|_{min,i}^{E}$ is the exact lower ratio bound of active power to active load in the i^{th} experiment, $\frac{P_{DER}}{P_L}\Big|_{min,i}$ is the estimated lower ratio bound of active power to active load from D^{2}NDZ, N_S is the number of experimental scenarios, m_i is the corresponding weight coefficient of a scenario. m_i should be increased if the probability of the i^{th} operation scenario increases [12].

III. Test Cases

A typical distribution feeder in Eversource Energy's service territory of Connecticut in the USA is used to validate D^{2}NDZ. It consists of 3717 sections and three PV arrays at different locations. Since the topology of an actual distribution grid is very complex, reasonable system reduction is necessary to accelerate system modeling, simulation and evaluation. Fig. 2 shows schematic one-line diagram of the equivalent feeder where the PV array is modeled in great detail. The high-fidelity of the reduced model in re-producing system dynamics and steady state behaviors has been thoroughly validated, which is omitted due to limited space.

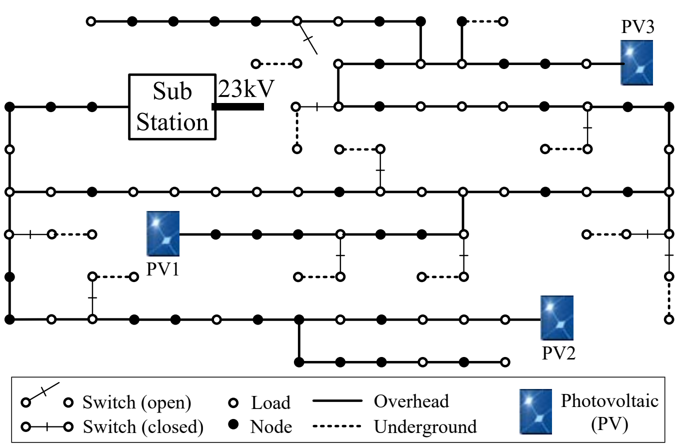

Fig. 2 A typical distribution feeder in Eversource Energy

A. Comparisons between D^{2}NDZ and the Simulation-Based Method

Comparisons of NDZs constructed by D^{2}NDZ and EMT simulations are shown in Fig. 3, where two cases are given as examples. In Case 1, only PV1 is integrated in the test feeder, whereas all three PV arrays are interconnected in Case 2. In both cases, the load percentages are set as: $P_I = 0$, $P_P = 50\%$, $P_C = 50\%$. Three critical islanding durations, 1s, 2s, 3s (i.e., clearing times in IEEE Standard 1547-2003), have been studied, which means that the NDZ corresponding to each islanding duration is formulated as four optimization problems, as shown in (27). Fig. 3 offers the following insights:

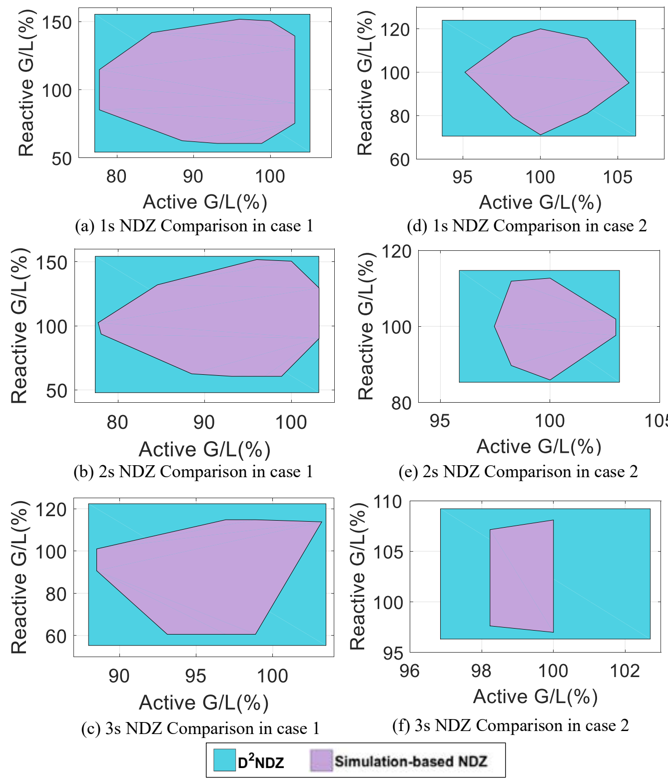

(a) 1s NDZ Comparison in case 1
(b) 2s NDZ Comparison in case 1
(c) 3s NDZ Comparison in case 1
(d) 1s NDZ Comparison in case 2
(e) 2s NDZ Comparison in case 2
(f) 3s NDZ Comparison in case 2

Fig. 3 Comparisons between D^{2}NDZ and simulation-based method

- NDZs obtained from D^{2}NDZ closely approach those from the EMT simulations within acceptable errors, meaning D^{2}NDZ is *effective*;
- Based on the optimized parameters, D^{2}NDZ can quickly estimate NDZs for any given feeder without numerous and time consuming EMT simulations, meaning D^{2}NDZ is *efficient*;
- An NDZ constructed by D^{2}NDZ is always more likely to be an over-approximation when compared with an NDZ obtained from EMT simulations, meaning D^{2}NDZ is *dependable*. This feature, in fact, is extremely important and helpful in practice, since it gives an early warning to utility engineers in advance when a feeder's operating point is approaching NDZ.

B. Impacts of DER Units on NDZ

The progressively deeper integration of DERs, especially power electronics interfaced units (e.g., PV and Battery), is significantly changing distribution grids' transient performance. Therefore, it is critically important to explore the impact of multiple DER units on NDZ. Fig. 4 shows the D^{2}NDZ results for two different cases. Case 1 compares the D^{2}NDZ results between the integration of PV and the integration of two PVs, whereas Case 2 compares the results between the integration of one PV and one battery and the integration of two PVs and one battery. Specifically, the battery's impacts should be calculated via h_L, h_H, l_L, l_H in (21)–(24). The following can be observed from Fig. 4:

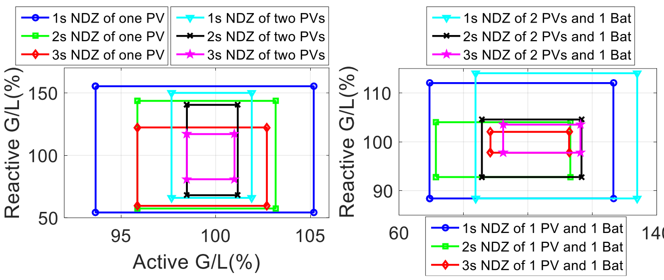

Fig. 4 Impacts of DER units on NDZ

- Under deep DER integration, e.g., when the ratio of active power to active load is around 100%, the more power-electronics-interfaced DER units a distribution feeder has, the smaller its NDZ would be.
  The reason is that the D^{2}NDZ boundary is largely related to the DER transient process which is mainly determined by DER controllers. It is basically infeasible to coordinately design their control parameters so as to seamlessly switch a feeder to operate in islanded mode.
- Power electronics interfaces decrease the baseline boundaries of NDZ, which is obtained when only the steady-state is considered (using (7) and (16)). For instance, the baseline NDZ of active power to active load for the case '3s NDZ of one PV' in Fig. 4 is $[77.44\%, 121\%]$, which is significantly larger than the overall NDZ results shown in Fig. 4.
  The reason is that low-inertia power electronic interfaces make the distribution feeder so sensitive to disturbances that their dramatic transient process can easily violate the volt/frequency requirements specified in IEEE Standard 1547 and thus can hardly sustain an island.
- The emergence of PV in a system brings about a small NDZ, which means adding low-inertial DERs in the generation mix,thus decreasing the boundaries of NDZ.

IV. Conclusions

A D^{2}NDZ approach is developed to evaluate the unintentional islanding risks in distribution networks. The primary NDZ is derived based on the ratio of active (reactive) power to active (reactive) load, and the impact of DER dynamics on the boundary of NDZ are then discussed and incorporated to the primary NDZ to establish the overall D^{2}NDZ. Parameters involved in D^{2}NDZ are determined through an optimization process, where a multiple scenarios-based objective function is designed to improve the robustness of the D^{2}NDZ method. Numerical examples are performed on a typical distribution feeder in Eversource Energy's service territory. Analyses and tests have confirmed the feasibility and effectiveness of D^{2}NDZ. Therefore, D^{2}NDZ is a practical, powerful, and efficient tool for planning, operating and protecting in distribution networks.

Appendix

Assuming the load resistances before and after islanding can be expressed as follows:

$$R = R_I + R_P + R_C,$$
$$R + \Delta R = (R_I + \Delta R_I) + (R_P + \Delta R_P) + (R_C + \Delta R_C),$$

Given P_I, P_P, P_C, the fractions between the corresponding resistances can be expressed as:

$$R_I : R_P : R_C = P_P P_C : P_I P_C : P_I P_P. \tag{28}$$

Note that $\Delta R_I = 0$, and constant power and current loads should satisfy the following conditions:

$$\frac{V^2}{R_P} = \frac{(V + \Delta V)^2}{R_P + \Delta R_P}, \tag{29}$$
$$\frac{V}{R_C} = \frac{V + \Delta V}{R_C + \Delta R_C}. \tag{30}$$

Then ΔR_P and ΔR_C can be expressed as follows

$$\Delta R_P = (2\mu + \mu^2) R_P = (2\mu + \mu^2)\frac{P_I}{P_P} R_I, \tag{31}$$

$$\Delta R_C = \mu R_C = \mu \frac{P_I}{P_C} R_I. \tag{32}$$

References

[1] T. Caldognetto, L. Dalla Santa, P. Magnone, and P. Mattavelli, "Power electronics based active load for unintentional islanding testbenches," *IEEE Transactions on Industry Applications*, 2017.

[2] Z. Ye, A. Kolwalkar, Y. Zhang, P. Du, and R. Walling, "Evaluation of anti-islanding schemes based on nondetection zone concept," *IEEE transactions on power electronics*, vol. 19, no. 5, pp. 1171–1176, 2004.

[3] Y. Jung, J. Choi, B. Yu, G. Yu, and J. So, "A novel active frequency drift method of islanding prevention for the grid-connected photovoltaic inverter," in *Power Electronics Specialists Conference, 2005. PESC'05. IEEE 36th*, pp. 1915–1921, IEEE, 2005.

[4] H. Vahedi and M. Karrari, "Adaptive fuzzy sandia frequency-shift method for islanding protection of inverter-based distributed generation," *IEEE Transactions on Power Delivery*, vol. 28, no. 1, pp. 84–92, 2013.

[5] S. Liu, S. Zhuang, Q. Xu, and J. Xiao, "Improved voltage shift islanding detection method for multi-inverter grid-connected photovoltaic systems," *IET Generation, Transmission & Distribution*, vol. 10, no. 13, pp. 3163–3169, 2016.

[6] X. Chen and Y. Li, "An islanding detection algorithm for inverter-based distributed generation based on reactive power control," *IEEE Transactions on Power Electronics*, vol. 29, no. 9, pp. 4672–4683, 2014.

[7] W. K. Najy, H. Zeineldin, A. H. K. Alaboudy, and W. L. Woon, "A bayesian passive islanding detection method for inverter-based distributed generation using esprit," *IEEE Transactions on Power Delivery*, vol. 26, no. 4, pp. 2687–2696, 2011.

[8] F. De Mango, M. Liserre, and A. Dell'Aquila, "Overview of anti-islanding algorithms for pv systems. part ii: Activemethods," in *Power Electronics and Motion Control Conference, 2006. EPE-PEMC 2006. 12th International*, pp. 1884–1889, IEEE, 2006.

[9] N. Lidula and A. Rajapakse, "A pattern recognition approach for detecting power islands using transient signals—part i: Design and implementation," *IEEE Transactions on Power Delivery*, vol. 25, no. 4, pp. 3070–3077, 2010.

[10] G.-K. Hung, C.-C. Chang, and C.-L. Chen, "Automatic phase-shift method for islanding detection of grid-connected photovoltaic inverters," *IEEE Transactions on Energy Conversion*, vol. 18, no. 1, pp. 169–173, 2003.

[11] "Interconnecting distributed resources with electric power systems," standard, IEEE Standard 1547-2003, 2003.

[12] C. Wang, Y. Li, K. Peng, B. Hong, Z. Wu, and C. Sun, "Coordinated optimal design of inverter controllers in a micro-grid with multiple distributed generation units," *IEEE Transactions on Power Systems*, vol. 28, no. 3, pp. 2679–2687, 2013.